DYNAMIC PARAMETERS AS DAMAGE INDICATORS FOR FIBRE REINFORCED MATRICES

N.B. Sørensen, Consulting Engineer
Rambøll A/S
Nørregade 7A,1165 Copenhagen K
Denmark

P.H. Kirkegaard, Assistant Professor
Aalborg University, Dept. of Build. Tech. and Struct. Eng.
Sohngaardsholmsvej 57, 9000 Aalborg
Denmark

ABSTRACT

The investigations reported in this paper look into the application of using measured changes in dynamic parameters to detect fatigue damage in concrete structures. Fatigue tests were performed as 4-point non-reversed load controlled bending tests on 50x50x500 mm un-notched beams. In the test the cyclic load was stopped after a certain amount of load cycles.The free-free beam was excited by a series of pulses introduced at the lower end of the beam by an impulse hammer. The acceleration of the beam was recorded and analysed by an Auto Regressiv Moving Average (ARMA) model. To indicate the damage process the development in dynamic parameters was studied as a function of n/N, i.e. the current number of cycles divided by the number of cycles to failure. In all it may be concluded that the first- and second-natural frequency seem to be a promising possible tool as indicator of the degradation process connected to the fatigue loading. Further, it seems to be impossible to use the modal damping ratio as indicator of fatigue damage development.

Keywords: Fibre reinforced matrices, Fatigue failure, Damage detection, ARMA - models, System Identification

1 INTRODUCTION

Fatigue failure can be interpreted as a result of accumulated damage. During repeated loading of concrete the internal structure of the material display permanent changes. The damage is known to be related to microcracking in the structures. The problem of fatigue analysis in both constant and variable amplitude loading, is to predict the accumulation of damage. The problem is related to the lack of knowledge about the progressive damage mechanism /1/.
As fatigue is associated with microcracking it would be obvious to express the damage development in terms of some kind of measure of cracking of the structure tested. But for practical purposes it

seems more appropriate to use some kind of "external" measure of damage. This is possible because changes in these "external" quantities are found to be related to the microcrack development during fatigue loading.
Based on the "external" measures of damage it may be possible to obtain

- information about the fatigue process expressed in terms of microcracking
- an indication of the immediate state of damage during a test
- a prediction of the fatigue life *(N)* during the test period (if possible)

Several methods have been used to follow the damage accumulation in plain concrete, e.g.:

- the ultrasonic pulse velocity method
- the acoustic emission method
- strain/deflection measurements

Among references dealing with damage development are /1/, /2/, /3/, /4/ and /5/. These references are all based on compressive fatigue tests. In /6/ damage development was studied in terms of midspan deflection in 4-point bending tests.
Recently, much research has been done with a vibrational based damage detection technique which does not need access to the structure for the investigator. A comprehensive review of the basic ideas in vibrational based inspection (VBI) of civil engineering structures might be found in /7/.
The motivation for doing these VBI tests is twofold. First, the use of dynamic parameters (eigenfrequencies and damping ratios) as damage indicators provides an alternative to the deflection measurements described in /6/. Second, the installation and use of an accelerometer is much simpler for practical purposes than the use of displacement transducers and/or strain gauges. The use of dynamic parameters as damage indicators is commonly seen in case of steel structures.
The idea behind the VBI method is based on the fact that all types of loading of a concrete structure may cause small (and maybe invisible to the naked eye) amounts of cracking and weakening of the structure. This damage will be accumulated and may cause a considerable decrease in the strength of the structure. This decrease in strength and stiffness affects the dynamic behaviour of the structure. It becomes "softer and softer". By measuring the response of the structure to real loadings or more well defined loadings provided by special loading arrangements it may be possible to observe changes in the dynamic response due to the degradation of the structure. These changes may be used as indicators of the damage development.
The tests in this paper should only be considered as a prelimenary study of the method since the structure consists of a small (50 x 50 x 500 mm) beam which is different from very complex real structures. But in case the method cannot be applied to this simple structure it seems to be meaningless to expand the tests to more complex conditions.
Even if the future will show that the method cannot be used to detect damage in real structures it may be used to detect damage in simpler fatigue tests.
The fatigue tests were performed as 4-point non-reversed load controlled tests on un-notched beams.
The parameter estimation is solved by using a time domain identification method (ARMA). In recent years the application of ARMA models to the description of structural systems has become more common, see e.g. /8/, /9/ and /10/ The structural time domain identification techniques using ARMA representation have been compared with frequency domain techniques in e.g. /11/. In this and other papers it has been documented that these ARMA time domain modelling approaches are superior to Fourier approaches for the identification of structural systems.

2 PREPARATION OF SPECIMENS

The test specimens were made of a high strength, fibre reinforced concrete material. The fibre content was 6 % by volume. The material was the matrix of Compact Reinforced Composite (CRC) - a fibre reinforced concrete with additional closely spaced main reinforcement. CRC is patented by Aalborg Portland. The composition of the CRC matrix is shown in table 1 for a batch of 27.5 litres. The fibres were Bekaert ø 0.40 x 12 mm of steel.
The total mixing time was 9 minutes. The time of vibration for the beams was close to 6 minutes. From each batch 12 beams of size 50 x 50 x 500 mm and three control cylinders of size 100 x 200 mm were cast in steel moulds.

Component	kg per 27.5 liter	weight % of cement
Binder (Densit)	25.0	100
Additional Silica Fume	0.788	3.30
Sand 0 - 1/4	4.533	18.3
Sand 1/4 - 1	9.194	36.8
Sand 1 - 4	18.440	73.8
Additional SPT	0.075	0.30
Water	4.071	16.3
Bekaert steel fibres	12.950	51.8

Table 1 Composition of 27.5 litres CRC matrix.

All specimens were covered by plastic and cured one day in the moulds at laboratory conditions followed by 7 days of curing at 45 °C. After this period the specimens were kept under laboratory conditions until the day of testing. The average compressive strength was close to 165 MPa with a scatter of 3 %. The average bending strength expressed in terms of the modulus of rupture was 24-25 MPa with a typical scatter of 5-6 %.No special preparation of the specimens was made before testing.

3 TEST PROCEDURE

3.1 Static Bending Tests

The static bending tests were performed in order to fix the loads for the fatigue tests.In order to take the variability into account more specimens from the same batch were tested. The tests were performed using the test equipment shown in figure 1.The test set-up consisted of an Instron load frame having a capacity of 500 kN in static tests and a hydraulic power supply. The tests were run from a personal computer (PC) on which the program *Series IX Automated Materials Testing System - version 5.31* by Instron was installed. The static tests were performed as displacement controlled 4-point bending tests. The tests were controlled by the piston displacement using the build-in LVDT. The displacement rate on the ascending branch and the first part of the descending branch were 0.2 mm/min. At a beam displacement of 2.2 mm the rate was increased to 1 mm/min.

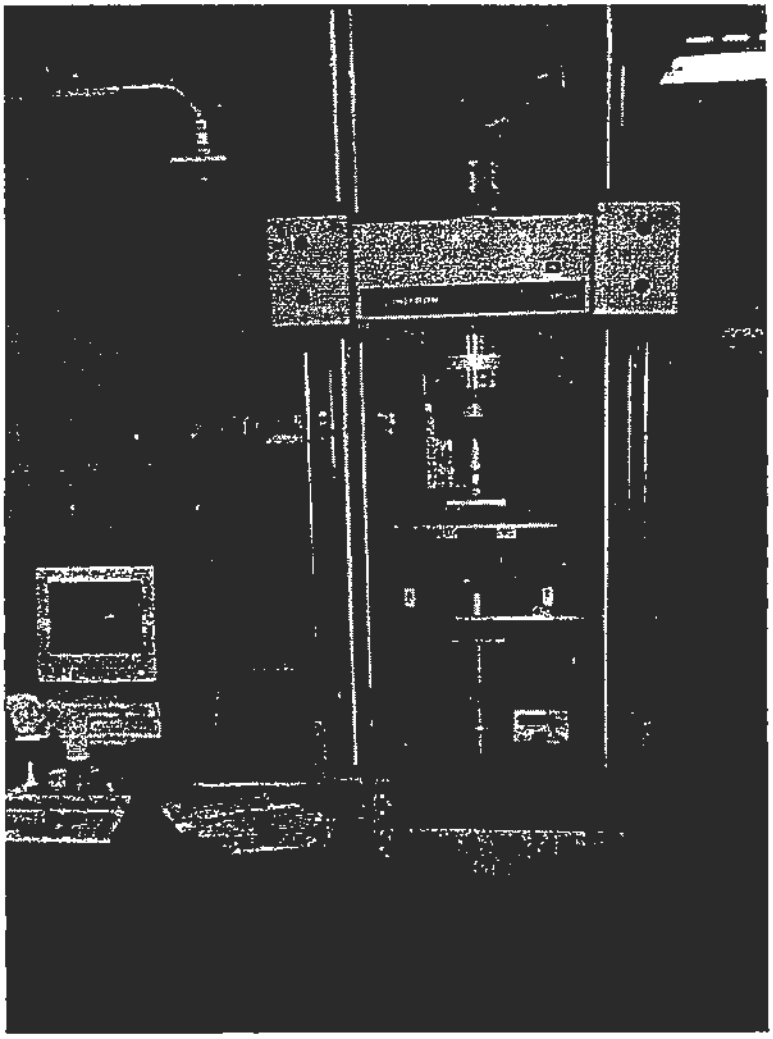

Figure 1 Test set-up for static tests. Picture from CBL, Aalborg Portland.

3.2 Fatigue Tests

The fatigue tests were performed with loads cycling between selected maximum- and minimum-load levels. The load levels were expressed as a fraction of the static strength on similar specimens (same material, age, geometry etc.). The load signal was sinusoidal with a frequency in the range of 0.3 - 3 Hz. The minimum load level, S_{min}, was 0.05 in all tests. The maximum load levels, S_{max} were selected in order to get lifetimes in the range of 100-50000 cycles.The fatigue tests were performed as load controlled 4-point bending tests.The set-up was identical to the set-up shown in figure 1. Initially, it was controlled that the load increased to the selected level within an appropriate amount of time, i.e. within one or two cycles. The tests were continued to failure.
The test programme was divided in two parts. The first part was performed in December 1994 at the Cement and Concrete Laboratory (CBL), Aalborg Portland. In this part 5 beams were tested. The second part was performed in March 1995 at CBL. In this part 3 beams were tested. The purpose of the tests was to study changes in dynamic parameters (eigenfrequencies and damping ratios) due to the cyclic load.

In the tests the cyclic load was stopped after a certain amount of load cycles. The beam was taken out of the set-up in figure 1 and a long string was attached to a hook glued to one end of the beam, see figure 2. By this procedure the beam was forced to vibrate under free-free conditions.
The free-free beam was excited by a series of pulses introduced at the lower end of the beam by a B&K 8202 impulse hammer. The acceleration of the beam was recorded by a single B&K 4370 accelerometer and a B&K 2635 charge amplifier. Before sampling the signal was low-pass filtered using an 8-pole Butterworth filter, type Rockland series 2000, model 2382.
The data acquisition system used in the project was based on a personal computer 386-40 MHz with an add-on A/D 16 bit simultaneous DT-2829 data acquisition board. The instrumentation for the dynamic parameter tests is shown in figure 2.

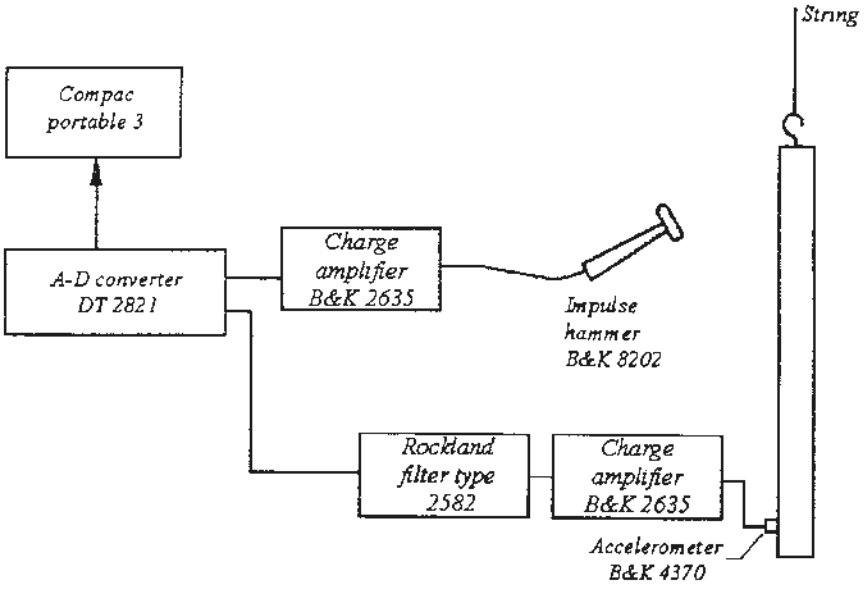

Figure 2 Instrumentation for the dynamic parameter tests.

After measurement of the vibrations the beam was installed in the set-up in figure 1 and the cyclic load was continued. At each test stop five acceleration time series were recorded, i.e. five estimates of eigenfrequencies and damping ratios could be determined at each test stop. In order to get a single value of the dynamic parameters at each stop the 5 estimates were combined according to the following expressions where $\sigma_{f,k}$ and $\sigma_{\zeta,k}$ are the standard deviation of the estimated eigenfrequency f_i and damping ratio ζ_i, respectively.

$$f_i = \frac{\sum_{k=1}^{5} \frac{f_{i,k}}{\sigma_{f_{i,k}}^2}}{\sum_{k=1}^{5} \sigma_{f_{i,k}}^{-2}} \quad , \quad \zeta_i = \frac{\sum_{k=1}^{5} \frac{\zeta_{i,k}}{\sigma_{\zeta_{i,k}}^2}}{\sum_{k=1}^{5} \sigma_{\zeta_{i,k}}^{-2}} \qquad (1)$$

3.3 Estimation of Dynamic Parameters using ARMA Models

Linear dynamic systems are generally described by continuous time domain ordinary or partially differential equations. Modern recording systems, however, are all digital and give measurements in discrete form. One commonly used approach to convert equations from continuous time domain to discrete time domain is the covariance equivalent approximation.
This means, if an ARMA(*2n,2n-1*) model is used for a stationary Gaussian white noise excited linear n-degree of freedom system it can be shown that the covariance of the response due to the ARMA model and that of the white noise excited structure will be identical, see e.g. /9/. Given a measured response $y(t)$ the ARMA(n_a,n_c) model is defined as

$$y(t) + a_1\, y(t-1) + \ldots + a_{n_a}\, y(t-n_a) = e(t) + c_1\, e(t-1) + \ldots + c_{n_c}\, e(t-n_c) \qquad (2)$$

where $y(t)$ is obtained by filtering the Gaussian white noise $e(t)$ through the filter described by the Auto Regressive polynomial, consisting of n_a AR-parameters a, and the Moving Average polynomial, consisting of n_c MA-parameters c_i. By introducing the following polynomials in the backward shift operator q^{-1}, defined as $q^{-j}\, y(t) = y(t-j)$

$$\begin{aligned} A(q^{-1}) &= 1 + a_1\, q^{-1} + \ldots + a_{n_a}\, q^{-n_a} \\ C(q^{-1}) &= 1 + c_1\, q^{-1} + \ldots + c_{n_c}\, q^{-n_c} \end{aligned} \qquad (3)$$

eq. (3) can be written in a more compact form as

$$y(t) = \frac{C(q^{-1})}{A(q^{-1})}\, e(t) \qquad (4)$$

The roots of $A(q^{-1})$ are the poles of the model whereas the roots of $C(q^{-1})$ are the zeroes. Assuming that the model is stable the poles are in complex conjugated pairs. The relationship between the poles p_j and the modal parameters is given by

$$p_j = e^{2\pi f_j T(-\zeta_j + i\sqrt{1-\zeta_j^2})} \qquad j = 1 \ldots n_a \qquad (5)$$

where f_j and ζ_j are the natural eigen-frequency and damping ratio of the jth mode. T is the sampling period. It is seen that each complex conjugated pair of poles corresponds to a simple-damped oscillator, see /10/

$$f_j = \frac{|\lambda_j|}{2\pi T}, \qquad \zeta_j = \frac{-Re(\lambda_j)}{|\lambda_j|} \qquad (6)$$

Setting $\lambda_j = \ln(p_j)$ the modal parameters are obtained from equation (7) where the quantity $|\lambda_j|$ denotes the modulus and $Re(\lambda_j)$ the real part of the complex number λ_j.
The parameters of the ARMA model are estimated by minimizing a quadratic error function, $V(\theta)$, defined as

$$V(\theta) = \frac{1}{2}\frac{1}{N-t_s+1}\sum_{t=t_s}^{N}\varepsilon(t,\theta)^2 = \frac{1}{2}\frac{1}{N-t_s+1}\sum_{t=t_s}^{N}(y(t) - \hat{y}(t,\theta))^2 \qquad (7)$$

$\hat{y}(t,\theta)$ is the predicted response and $t_s = \max(n_a,n_c)+1$. To calculate the parameter estimates using a numerical minimization method must be chosen, see e.g. /12/.
In order to deal with the order of the ARMA model Akaike, /13/, suggested an Information Theoretic Criterion (AIC) of the type

$$AIC = \log[(1 + \frac{2n}{N})\cdot V(\theta)] \qquad (8)$$

where N is the number of data in the time series, n is the number of parameters. The AIC criterion penalizes using too high model orders, i.e. their value may increase with increasing model order. The model structure giving the smallest value of the criterion is selected.
An important characteristic of ARMA-models is that it is possible to get unbiased estimates of the AR-parameters, e.g. /8/, where estimates of the variances of the estimated parameters can be estimated by the Cramer-Rao lower bound, e.g. /13/.
Model validation is the final stage of the system identification procedure. In fact model validation overlaps with model structure selection. Since the system identification is an iterative process various stages will not be separated: models are estimated and the validation results will lead to new models etc. Model selection involves the selection of the form and the order of the ARMA model, and constitutes the most important part of the system identification. Model validation is to confirm that the model estimated is a realistic approximation of the actual system. A throughout description of the problem of model selection and validation is given in /12/. One of the dilemmas in the model validation is that there are many different ways to determine and compare the quality of the estimated models. First of all, the subjective judgement in the model validation should be stressed. It is the user that makes the decision based on numerical indicators. The variance of the parameter estimates can be such an indicator.
It is also important to check whether the model is a good fit for the data recording to which it was estimated. Simulation of the system with the actual input and comparing the measured output with the simulated model output can also be used for model validation. One can also compare the estimated transfer function with one estimated by FFT. Statistical tests of the prediction errors are also typically used numerical indicators in model validation.

4 EXPERIMENTAL RESULTS

4.1 General

In this chapter the results from the experimental investigations are presented and discussed. In Appendix A it is explained how the ARMA-model was selected and validated. The estimated

eigenfrequencies and damping ratios are presented and discussed in section 4.2. The parameters are estimated by using the MATLAB programme, see /15/.
Details about the tests are given in table 2.

Beam no.	S_{max}	frequency (Hz)	lowpass (Hz)	f-sample (Hz)	fatigue life (cycles)	model order
1	0.88	0.3	1500	3000	806	ARMA(4,3)
2	0.92	0.3	1500	3000	4	*
3	0.92	0.3	1500	3000	89	ARMA(4,3)
4	0.84	3.0	3000	6000	3575	ARMA(6,5)
5	0.88	0.3	3000	6000	399	ARMA(6,5)
6	0.88	3.0	3000	6000	16894	ARMA(6,5)
7	0.88	1.0	3000	6000	280	ARMA(6,5)
8	0.88	3.0	3000	6000	19756	ARMA(6,5)

Table 2 Details about the tests. Frequencies in Hz. * mean that no analysis was performed because the beam failed after 4 cycles.

4.2 Test Results

In this section the development in the dynamic parameters due to cyclic loading will be studied in further details. From these results it may be possible to get more information about what actually happens when a specimen (beam) is exposed to cyclic loading. Further, the measurement of parameters that may be related to the developed damage may be used to predict the actual state of the "structure" at a given time in the load process. In time one could hope that the information obtained during the fatigue process could be used to evaluate whether the structure is "suffering" because of the load. In the future that kind of information may be used to predict the remaining lifetime of the structure and to say whether it is necessary to repair the structure. However, at present it seems too optimistic to believe that the results can be applied to more than "just" explain what is happening during the fatigue loading process.
To indicate the damage development the dynamic parameters were studied as a function of n/N, i.e. the current number of cycles divided by the number of cycles to failure.
During the tests the fatigue process was studied by the author by watching the beams using the naked eye and a magnifying glass. By this process it was observed that the beams went through a "multiple cracking" state until the damage became localized in one single major crack. Most of the cracks could only be observed using a magnifying glass. Often 10 cracks (some very small) were observed in the zone between the points of load application. For high load levels the major crack was developed almost immediately and it was very difficult to separate the "multiple cracking" process and the development of the major crack.
For all tests the major crack was vertical and situated in the zone between the points of load application. The failure was due to fibres being "pulled out" of the matrix. The fibre "pull-out" mechanism was easily identified by watching the major crack in the magnifying glass. At the bottom of the beam fibres were observed to be pumping in and out of the matrix.

In the present section special attention will paid to the development in the two lowest natural frequencies (f_1 and f_2) and the two lowest damping ratios (ζ_1 and ζ_2) during the fatigue life. In some specimens only the lowest frequency and damping ratio were determined.
Instead of discussing the individual test results it was decided to consider all test specimens together. First, the development in the first natural frequency is studied for all the beams. The results are shown in figure 3.

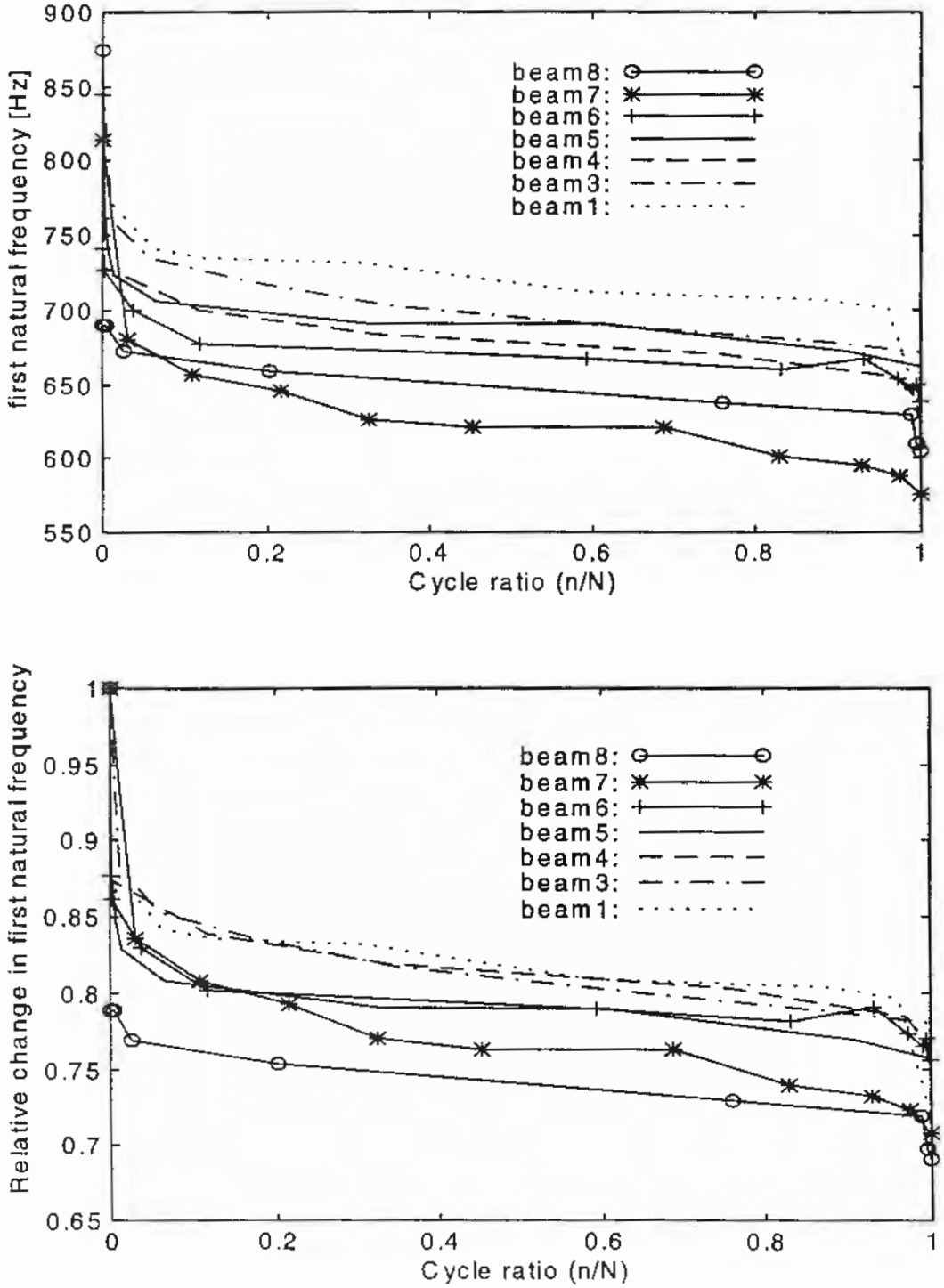

Figure 3 Development in first natural frequency in absolute values and in relative values.

The figure 3 contains information about the development in the absolute value as well as the relative value of f_1. Here the relative value means the current value divided by the initial value. All results are expressed in non-dimensional time in terms of the cycle ratio *n/N*.
Expressed in terms of absolute values the initial seems to be in the range of 800-900 Hz.
Generally, the development in the first natural frequency seems to consist of three stages. The first stage is very short as it lasts less than 5 % of the total fatigue life. During this stage an abrupt decrease in the frequency is observed. The frequency at the end of the first stage is typically in the range of 77-87 % of the initial value.
The second stage is characterized by a gradual and stable development in the first natural frequency. This stage ends very close to failure. Typically *n/N* was in the range of 0.95-0.99 at the end of this stage. The third stage occuring just before failure is characterized by a very abrupt decrease in f_1.
The value of f_1 at the end of the second stage was typically in the range of 73-83 % of the initial value. The trend indicated that the specimens with the lowest relative frequencies at the end of the first stage also have the lowest relative frequencies at the end of the second stage.
Generally, it was not possible to identify a unique relation between the number of cycles to failure and e.g. the relative decrease in f_1 at the end of the first- and/or the second- stage. However, there may be a tendency to a larger decrease for specimens having longer fatigue lives.
In all it may be concluded that the first natural frequency seems to be a promising possible tool as an indicator of the degradation process connected to the fatigue loading.
Next, the development in the second natural frequency is studied for the beams where the second mode was identified (beams 4-8). The results are shown in figure 4. The figure contains information about the development in the absolute value as well as the relative value of f_2. Here the relative value means the current value divided by the initial value. All results are expressed in non-dimensional time in terms of the cycle ratio *n/N*.
Expressed in terms of absolute values the initial value seems to be in the range of 2150-2250 Hz.
Generally the development in the second natural frequency seems to consist of three stages. The first stage is very short as it lasts less than 5 % of the total fatigue life. During this stage an abrupt decrease in the frequency is observed. The frequency at the end of the first stage is typically in the range of 87-93 % of the initial value, i.e. the decrease was much less than observed for the first natural frequency.
The second stage is characterized by a gradual and stable development in the second natural frequency. This stage ends very close to failure. Typically *n/N* was in the range of 0.95-0.99 at the end of this stage. The third stage occuring just before failure is characterized by a very abrupt decrease in f_2. The value of f_2 at the end of the second stage was typically in the range of 83-90 % of the initial value. The trend indicated that the specimens with the lowest relative frequencies at the end of the first stage also have the lowest relative frequencies at the end of the second stage although the results were less stable than for the first natural frequency.
As for the first natural frequency it was not possible to identify a unique relation between the number of cycles to failure and e.g. the relative decrease in f_2 at the end of the first- and/or the second- stage.
In all it may be concluded that the second natural frequency seems to be a promising possible tool as an indicator of the degradation process connected to the fatigue loading. But as mentioned previously the development in the second natural frequency seems to be less stable and gradual.
The previous analysis of the first- and second- natural frequencies seemed to indicate a larger decrease in the first natural frequency. In order to examine this subject a little further the relative changes in the first- and second- natural frequencies are shown in figure 5.
The mentioned tendency is clearly illustrated. While an almost similar development is seen in the second stage the initial decrease in the first natural frequency is seen to be more pronounced than the decrease in the second natural frequency. For practical purposes it means that the first natural frequency provides a more reliable indication of damage developement due to fatigue loads. If this

conclusion remains correct for high cycle fatigue it means that it may be possible at an early stage to predict whether or not there seems to be a risk of fatigue failure in time. However, to make any conclusions about the behaviour of the dynamic parameters in the high cycle region and for "run-out" specimens further tests should be performed.

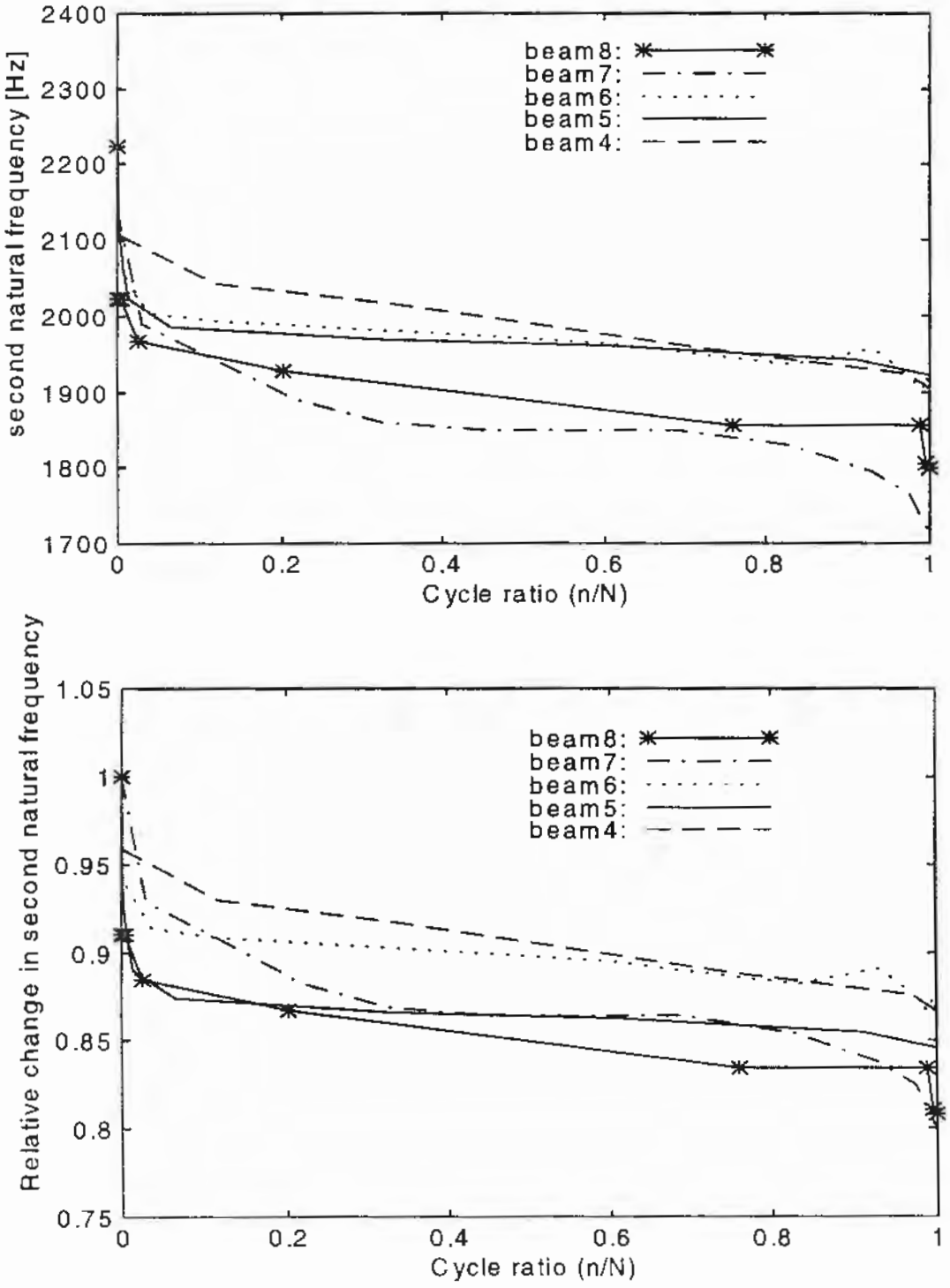

Figure 4 Development in second natural frequency in absolute values and in relative values.

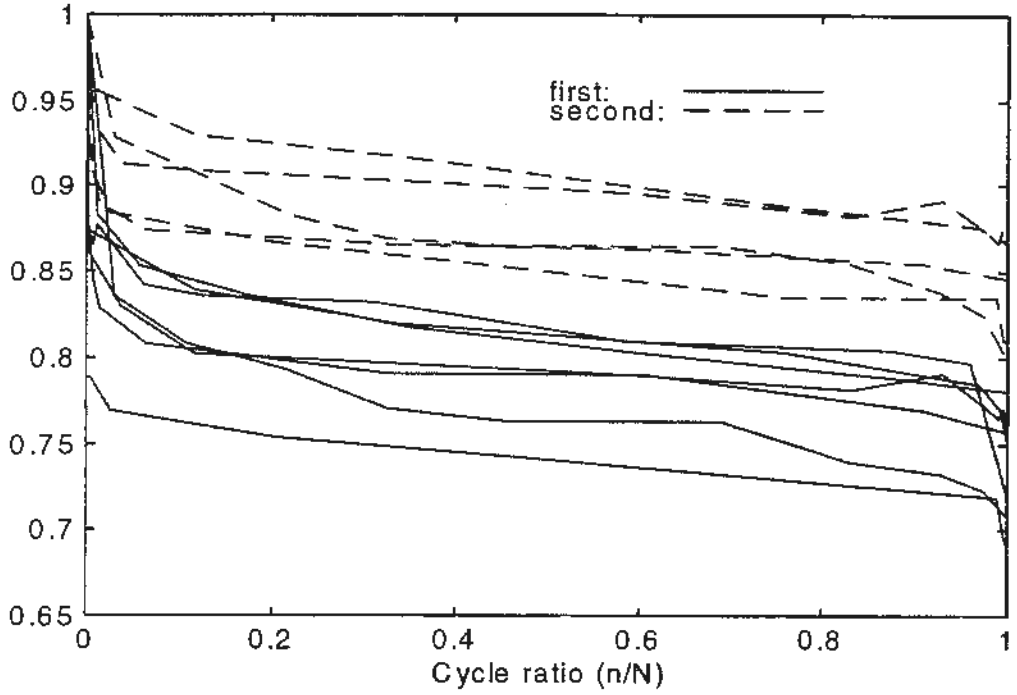

Figure 5 Relative development in first- and second- natural frequency.

Another important conclusion that can be derived from figure 5 is the importance of a "virgin state" measurement, i.e. a determination of the dynamic parameters in the undamaged situation. If there is a risk of fatigue failure a major part of the total damage seems to develop early in the process. If the first measurement was performed after a few per cent of the number of cycles to failure the changes in the dynamic parameters based on following measurements will be less pronounced.
In the following a few comments will be made concerning the modal damping ratios as damage indicators. Both first- and second- modal damping ratio will be examined at the same time.
Generally, it is very difficult to find any definite trends in the development in terms of n/N. Therefore, it was decided not to study these parameters further. At present the only conclusion seems to be that it is impossible to use the modal damping ratios as indicators of fatigue damage development. The conclusion about modal damping ratios as unreliable damage indicators has often been met in the literature, see e.g. /7/.The first modal damping ratio seems to be in the range of 0.01 to 0.02 although considerable scatter is observed. The second modal damping ratio seems to be in the range 0.005 to 0.012.

5 CONCLUSIONS

This paper deals with damage detection in flexural low-cycle fatigue tests as special attention was paid to dynamic parameters (eigenfrequencies and modal damping ratios). The tests were performed on beams made of CRC matrix material.To indicate the damage process the development in dynamic parameters was studied as a function of n/N, i.e. the current number of cycles divided by the number of cycles to failure. Generally, it was not possible to identify a unique relation between the number of cycles to failure and e.g. the relative decrease in f_1 and f_2 at the end of the first- and/or the second-

stage. However, there may be a tendency to a larger decrease for specimens having longer fatigue lives.In all it may be concluded that the first- and second- natural frequency seem to be a promising possible tool as indicators of the degradation process connected to the fatigue loading. However, the development in the second natural frequency seems to be less stable and gradual.

While an almost similar development in the relative changes in the first- and second- natural frequencies is seen in the second stage the initial decrease in the first natural frequency was found to be more pronounced than the initial decrease in the second natural frequency. For practical purposes it means that the first natural frequency provides a more reliable indication of damage developement due to fatigue loads. If this conclusion remains correct for high cycle fatigue it means that it may be possible at an early stage to predict whether or not there seems to be a risk of fatigue failure in time. However, to make any conclusions about the behaviour of the dynamic parameters in the high cycle region and for "run-out" specimens further tests should be performed.
The fact that the lower natural frequency is more sensible to damage development may be explained by the fact that the damage is developed close to a peak in the first mode shape while the second mode shape has a "zero" at the same position. This conclusion has been motivated by FEM studies in /18/.
For both first- and second- modal damping ratio it is very difficult to find any definite trends in the development in terms of n/N.
Even though valuable information has been obtained in the present paper a lot of questions of vital importance still have to be investigated in the future in order to be able to use the method for practical purposes. Among the subjects that have not been covered in the present study are:

- tests of longer duration, including "run-out" tests
- dependence of the test set-up used to determine the dynamic parameters
- the applicability of the method in real structures
- the relative importance of changes due to cyclic loads compared to changes from
  - other loadings
  - environmental conditions (temperature, humidity etc)
  - connections in more complicated structures

ACKNOWLEDGEMENT

The present work was made in connection with the BriteEuRam Fellowship Damage control of CRC structures (Contract N° BRE2.CT94.3082, Project BE-6015). This financial support is gratefully acknowledged.

REFERENCES

/1/ Jinawath, P.: "Cumulative fatigue damage of plain concrete in compression". Ph.D. thesis, University of Leeds, 1974.

/2/ Holmen, J.O.: "Fatigue of concrete by constant and variable amplitude loading". Bulletin No. 79-1, Division of Concrete Structures, Norwegian Institute of Technology, University of Trondheim, 1979; 218 pp.

/3/ Petkovic, G.: "Properties of concrete related to fatigue damage with emphasis on high strength concrete". Doktor Ingeniöravhandling 1991; 35, Institutt for Betongkonstruksjoner, Trondheim, Norway, 1991.

/4/ Sørensen, N.B.: "Rapport 6.4: Effect of maximum stress, stress range, stress ratio and stress rate on fatigue behaviour of plain concrete subject to uniaxial constant-amplitude compression". Instituttet for Bygningsteknik, AUC, Feb. 1992.

/5/ Sørensen, N.B.: "Rapport 6.7: The fatigue process in low- and high-cycle fatigue". Instituttet for Bygningsteknik, AUC, Feb. 1993.

/6/ Sørensen, N.B.: "Low-cycle fatigue tests of CRC beams". Report no. 3 in the BriteEuRam Fellowship "Damage control of CRC structures"; February 1995.

/7/ Rytter, A.: "Vibrational Based Inspection of Civil Engineering Structures".Ph.D.Thesis, Aalborg University, 1993.

/8/ Pandit, S.M & S.M. Wu: "Time Series and System Analysis with Applications". John Wiley and sons, 1983.

/9/ F. Kozin & H. G. Natke: "System Identification Techniques. Structural Safety". Vol. 3, 1986.

/10/ Safak, E.: "Identification of Linear Structures using Discrete-Time Filters". Journal of Structural Engineering, Vol. 117, No. 10, 1991.

/11/ Davies, P., & J. K. Hammond: "A Comparison of Fourier and Parametric Methods for Structural System Identification". Journal of Vibration, Acoustics, Stress and Reliability in Design. Vol. 106, pp.40-48, 1984.

/12/ Ljung, L.: "System Identification - Theory for the User". Prentice Hall, Englewood Cliffs, 1987.

/13/ Akaike, H.: "Fitting Autoregressive Models for Prediction". Am. Inst. Stat. Math., Vol. 21, pp. 243-347, 1969.

/14/ Kirkegaard, P.H.: "Optimal Design of Experiments for Parametric Identification of Civil Engineering Structures". Ph.D-Thesis, Aalborg University 1991.

/15/ "PC-MATLAB for MS-DOS Personal Computers". The Math Works, Inc., 1989.

/16/ Knudsen, T.: "A New Method for Estimating ARMAX Models". SYSID94,Copenhagen, 1994.

/17/ Sørensen, N.B.: "Dynamic Parameters as Damage Indicators for CRC ". Report no. 4 in the BriteEuRam Fellowship "Damage control of CRC structures"; April 1995.

/18/ Kirkegaard, P.H. & A. Rytter: "The use of Neural Networks for Dmage Detection and Location in s a Steel Member". Presented at the 3'rd international conference in the application of artificial intelligence to civil engineering structures. CIVIL-COMP 1993, Edinburgh, August 17-19 1993.

APPENDIX A:

Selection and Validation of ARMA-model

For each of the beams in table 2 an appropriate ARMA-model was selected. Only results from beam no. 5 will be presented. The selection and validation procedure were used on various damage states (each test stop corresponds to a damage state) and time series connected to the beam. In figure A.1 the AIC criterion, (8), is plotted as a function of the model order for beam no. 5, damage state no. 0 and time series no. 1. From figure 3 an ARMA(6,5) was selected for beam no. 5.

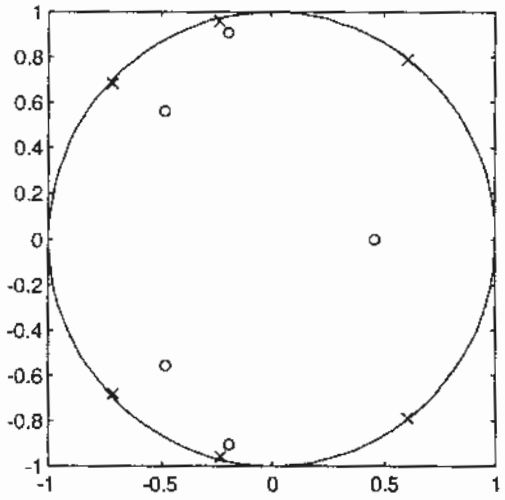

Figure A.1 AIC-criterion as a function of the model order, n.

As a further validation of this choise figure A.2 shows a plot of the poles (x) and zeros (o). It is seen that all the poles and zeros are inside the unit circle in the complex plane. The poles and zeros are given with confidence regions corresponding to three standard deviations. If these regions overlap, a lower model order would have been appropriate, since this is a result of a near pole-zero cancellation in the dynamic model indicating that the model order is too high.
The most dominant mode of the system is the one corresponding to the pole closest to the unit circle

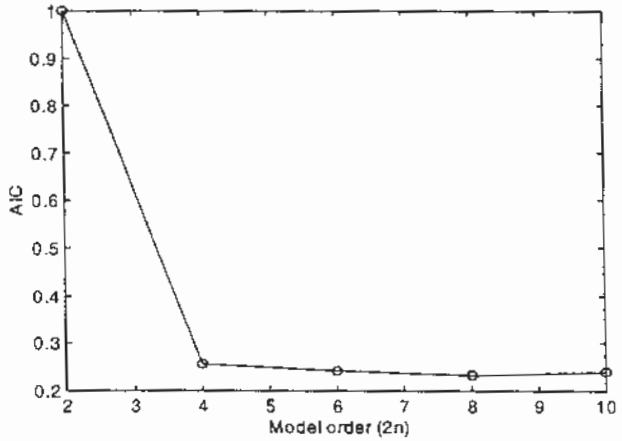

Figure A.2: Pole-Zero plot. x and o indicate poles and zeros, respectively.

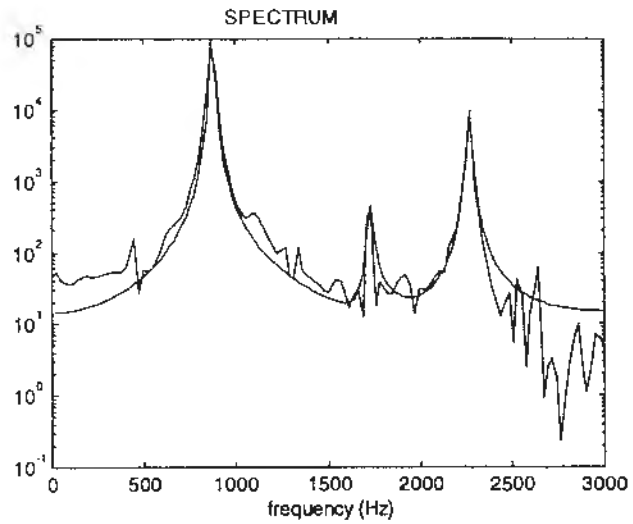

Figure A.3 Comparison of direct estimated spectrum and spectrum obtained from the AR-MA-model (smoothed-line).

Further, the match of the power spectrum obtained by a Fast Fourier Transformation and the spectrum obtained from the ARMA-model are shown in figure A.3. The figure A.3 shows a good match as both of the lowest eigenfrequncies are identified. Next the residuals of the identification are checked. Residuals are defined as the difference between the model output and the recorded output signal. In order to have a valid identification, the residuals should be a white-noise sequence. The plot of the autocorrelation of the residual time series is given in figure A.4.
Further a 99% confidence interval is indicated by the two straight lines. In case of white-noise residuals the autocorrelation function should be within these levels except for the zero lag. In /16/ it is emphasized that few outcrossings may be observed without having to neglect the model. The present results clearly indicate that the white-noise assumption is fulfilled.

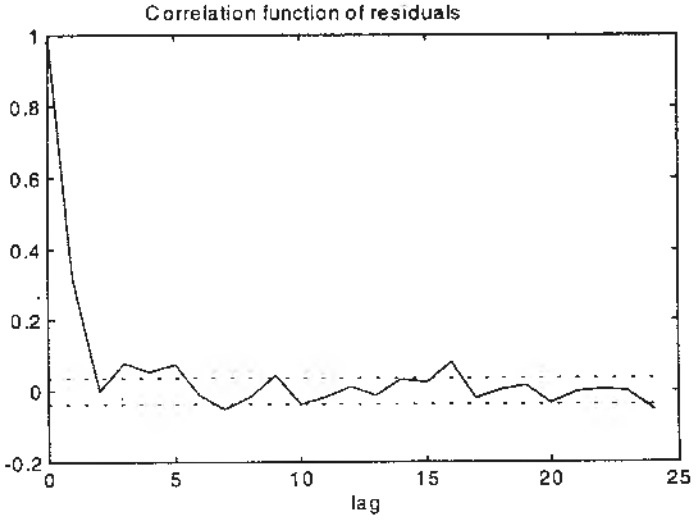

Figure A.4 Autocorrelation of the residual time series.

In /17/ more details about the selection and validation process are given.
For all tests where the two lowest eigenfrequencies could be identified, i.e. for tests with a sampling frequency of 6000 Hz, see table 2, the appropriate model was found to be ARMA(6,5). For the remaining tests only the lowest eigenfrequency could be identified and the appropriate model was ARMA(4,3).